ELSEVIER

Surface Science 438 (1999) 261–270

surface science

www.elsevier.nl/locate/susc

Excitation of vibrational modes of adsorbates with the scanning tunneling microscope: many-orbital theory

N. Mingo *, K. Makoshi

Faculty of Science, Himeji Institute of Technology, Kamigori, Hyogo 678-1297, Japan

Abstract

We derive theoretical expressions for taking into account inelastic tunneling effects in the current of a scanning tunneling microscope (STM), and relate them to the event rate of current-induced processes like desorption, rotation or dissociation of adsorbed molecules. In a realistic case, the current involves tunneling through many hybridized channels, and also several different modes can be excited simultaneously. Our scheme provides a tool to deal with such a general case. The theory presented allows us to predict vibrational-mode excitation of adsorbates, and calculate event rates. A model calculation is performed illustrating the capabilities of the calculational scheme, to obtain event rates as a function of the STM tip position ('inelastic image' of the adsorbate) and the bias. New features associated with the many-orbital character of the coupling are reported.

Keywords: Adsorption; Green's functions; Inelastic tunneling; Linear combination of atomic orbitals; Molecule manipulation; Scanning tunneling microscope; Vibrational modes

1. Introduction

Recently, several experiments have been done which show the importance of the inelastic interaction of tunneling electrons with adsorbed molecules in the scanning tunneling microscope (STM) as a mechanism for adsorbate manipulation. Different kinds of phenomena, namely molecule desorption and diffusion [1], dissociation [2] or rotation [3–5], have been shown to rely on the same basic process. According to Refs. [6,7], two ranges exist. They have been called the 'coherent' and the 'incoherent' mechanism. The coherent mechanism takes place when a single electron is able to inelastically excite the vibrational mode(s) from its ground state to its nth level, when the desorption, dissociation or diffusion (rotation) takes place. In this case, the vibrational mode's de-excitation time via substrate phonons, γ, must be fast compared with the inverse of the inelastic current.

The incoherent mechanism occurs when the inelastic current is high enough compared with γ^{-1}. This mechanism has also been called 'ladder climbing', because each electron is able to excite just one vibrational level. This mechanism is the one proposed by Avouris et al. [8,9] in their studies of xenon-induced desorption.

The main feature of the coherent mechanism is that it gives rise to a linear dependence of the desorption rate (or dissociation, or induced rotation) on the current. On the other hand, the incoherent (or multi-electron) mechanism predicts a power of N dependence on the current, N being the number of bound vibrational levels inside the

* Corresponding author. Fax: +81-7915-8-0151.
E-mail address: natalio@sci.himeji-tech.ac.jp (N. Mingo)

0039-6028/99/$ – see front matter
PII: S0039-6028(99)00579-8

well. Both mechanisms take place for the same system. The cross-over of both ranges occurs when the inelastic current is comparable with γ^{-1} [6,7].

In this paper we focus on the coherent process, which is the dominant one in the experiments cited. Several theoretical works have been published on this topic. The model of Persson and Baratoff [10] provided a main conceptual tool that has led further work. Semi-classical wave-packet dynamics have been used to analyze the experiments in Ref. [1], following the theory proposed by Gadzuk [11,12]. A quantum treatment has been given in [7], and used to analyze results of Refs. [2–5]. Also, ab initio calculations have included an electron–vibration coupling term to analyze experiments on induced desorption [13]. However, all these works are still based in the 'one resonance + one mode' model. Since any realistic case involves a complicated multi-orbital electronic structure, it is clearly necessary to go beyond the one resonance model, attacking the problem directly from a general Hamiltonian. Furthermore, in general there are several molecular modes that can be excited by the inelastic electronic interaction. We incorporate these two features in our formalism. One advantage of our many-orbital approach is that it permits one to obtain desorption (or dissociation or rotation) rates as a function of the tip's position. This enables calculation of spatially resolved rates, which can be compared with experimental ones. In the Appendix, we show how previously published expressions are recovered when we go to the one resonance limit case.

Regarding inelastic currents, a many-orbital approach has also been given in Ref. [14]; however, the model treated there just includes a single vibrational mode. We propose a Green's functions formalism which provides a simple way to calculate the general case of simultaneous excitation of several modes.

2. Multichannel theory of inelastic STM conductance

The general theory of elastic currents in the STM has been extensively studied. Linear combination of atomic orbitals (LCAO) methods are very well suited to combine quantum chemistry with theoretical surface physics techniques in order to study under a common framework both STM currents and the chemical interactions of the system [15]. Therefore, for conceptual simplicity, in what follows we shall assume an LCAO language. Nevertheless, the reasonings will remain valid independently of the particular representation chosen.

In the Appendix we derive non-perturbative expressions for the tunneling current. In this section we show how those expressions are used to calculate jointly both elastic and inelastic currents. To this end, we first set up the total Hamilonian, including the coupling between electrons and the vibrational modes of the adsorbate. Then we transform the system into a purely electronic one, where we can use Green's functions techniques to obtain the elastic and inelastic conductances in a non-perturbative way.

2.1. Coupling of electrons with the vibrational modes of the molecule

Usually, the electron–vibration coupling term is included in the Hamiltonian as [10]:

$$\delta\epsilon(\hat{V}^{+}+\hat{V})\hat{C}_a^{+}\hat{C}_a, \tag{1}$$

where the interaction takes place at site a, and $\hat{V}^{+}$ and $\hat{V}$ are the creation and destruction operators of the vibrational mode. However, if we consider the vibration in detail, we must take into account that the hoppings between pairs of atoms are changing. Therefore, at least two orbitals (in the limiting case of one orbital per atom) are involved in the interaction. In general, if one of the resonances is much closer to the Fermi level, it will be more important than the others in the tunneling process, so we recover the previously studied single resonance case of Ref. [10].

According to Ref. [10], $\delta\epsilon$ corresponds to:

$$\left.\frac{\partial E}{\partial R}\right|_{R=R_0}\Delta R, \tag{2}$$

where $\Delta R=(2m^{*}\Omega)^{-1/2}h/2\pi$ is related to the mean value of the displacement of the first excited state from the equilibrium position R_0, and E is the energy of the resonant level. Since, in the general

case, there is more than one resonance involved in the coupling process, we must extend the concept of $\delta\epsilon$ to a matrix:

$$\underline{\underline{\delta\epsilon}} = \frac{\partial H}{\underline{\underline{\partial R}}}\bigg|_{R=R_0} \Delta R, \tag{3}$$

so the electron–vibration coupling will be expressed by:

$$(\hat{V}_\mu^+ + \hat{V}_\mu)\sum_{i,j} \delta\epsilon_{ij}^{(\mu)} \hat{C}_i^+ \hat{C}_j, \tag{4}$$

where index μ labels the different vibrational modes. Obviously, i and j belong only to the atoms involved in the vibration, whose relative distances are varying. Matrix (3) contains all the information about the electron–vibration coupling at the adsorbed molecule.

2.2. Equivalent electronic Hamiltonian

As we show in the Appendix, the movement of an electron in the Hamiltonian previously described can be transformed in an equivalent system, where the excited vibrational state is represented by the electronic Hamiltonian $\boldsymbol{H}_2 = \boldsymbol{H}_1 + \Omega \boldsymbol{I}$, and the two Hamiltonians are coupled through the coupling matrix $\boldsymbol{\delta\epsilon}$. In such a way, when the electron enters the coupling region (see Fig. 1), it can release an energy Ω to the vibration, exciting one mode. The electron can similarly excite the vibration to the next vibrational level. So, another parallel system with energies shifted by 2Ω has to be coupled, and so on. H_{n-1} couples to H_n via:

$$\delta\epsilon_n = \frac{\partial \underline{\underline{\epsilon}}}{\partial R}\bigg|_{R=R_0} \langle n-1|X|n\rangle \propto \Delta R\sqrt{n},$$

where $\langle n-1|X|n\rangle$ is the matrix element of the vibrational coordinate's operator connecting the vibrational quantum states n and $n-1$.

In the case of several different modes coupling with electrons, the parallel subsystems are coupled in the way depicted in Fig. 1. A lattice-like pattern is formed, where each combination of final vibrational modes of the molecule corresponds to one knot in the lattice. Fig. 1 shows the example of two different modes, which can be excited up to two levels before desorption or diffusion of the molecule takes place.

2.3. Obtention of the currents

The system depicted in Fig. 1 is now easily interpreted. We shall consider that the electron finds the molecule in its ground state, and leaves it in some combination of excited states. Therefore, electrons are entering through branch A, which is considered the emitter. One can compute the amount of these electrons that are exiting through each of the different branches. Current entering through A and exiting through C constitutes the elastic current, I_0; i.e., the molecule remains in its ground state. Those exiting through D constitute the I_1 (in the notation of [7]). The index stands for the corresponding exit branch, and means the number of levels of the mode that have been excited. In the case of two different modes interacting with the electrons, we shall use the notation $I_{n,m}$, where n and m are the number of levels of each mode that are excited, and denote the branch through which current is exiting. In general, we must set as many indexes as modes are included in the electron–vibration (e–vib.) Hamiltonian.

The way of calculating the different $I_{n,m,l,\ldots}$ as a function of the Green's functions of the tip and the sample, and the e–vib. coupling matrices, are explained in the Appendix.

In general, some correlation between electrons would be expected due to the coupling with the vibration. The easiest way to treat such a correlation is to assume that subsystem B has also a small occupancy, being part of the emitter. Such an occupancy is given by Avouris et al.'s expression for the level's population [8,9]. However, in the calculations presented, we shall assume that the molecular relaxation time, γ, is small enough compared with the inverse of the total current, which means that electrons entering through B are negligible (in other words, the coherent mechanism is dominant, in the terminology of Ref. [7]).

3. Calculation

We analyze the model depicted in Fig. 2. The model allows us to investigate the features and

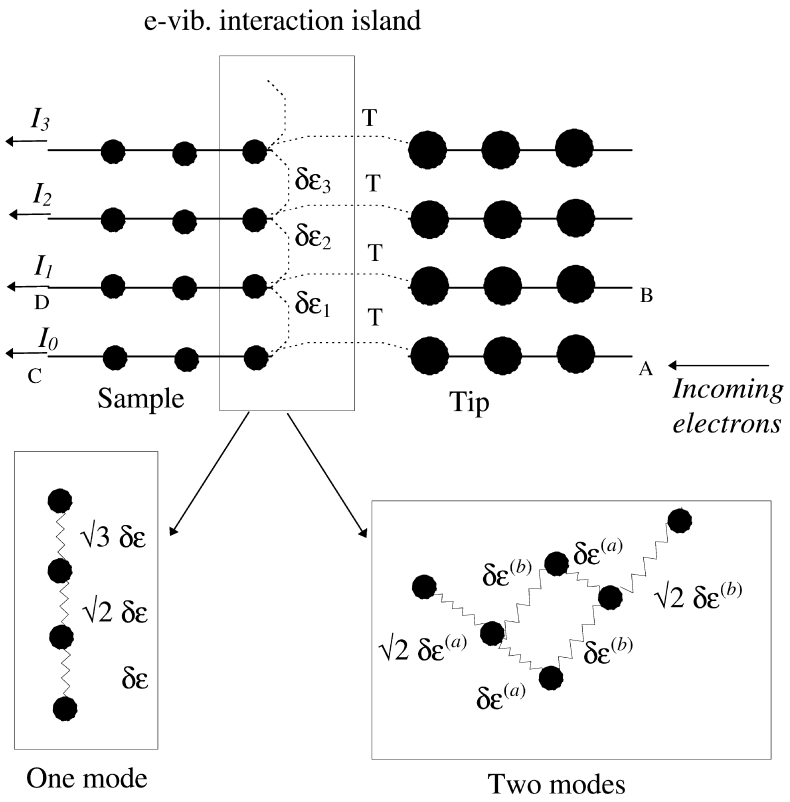

Fig. 1. Purely electronic Hamiltonian equivalent to the electron–vibration coupled Hamiltonian. One dot represents the group of orbitals involved in the interaction. The couplings between branches are matrices. Below the general picture we show two examples for the interaction island, with coupling to one or two different vibrational modes. In general, the case of coupling to N different vibrational modes will be represented by an N-dimensional graph.

capabilities of the method proposed, and its adequacy for studying more realistic problems.

The sample is modeled as three atoms. Two of them, representing the surface adsorption site, are attached to four-neighbor Bethe lattices, included as a self-energy in the Hamiltonian. This self-energy accounts for the bulk density of states [16]. The third one represents the adsorbate. Each atom is composed of a single S orbital. The energy levels are set at zero for the substrate atoms, and also the Fermi energy, E_F, equals zero. The adsorbate's energy level is set at $E_a = +1$ eV. Hopping matrix elements between the adsorbate and its neighbors are $T = -0.5$ eV. The hoppings between substrate atoms (including those in the Bethe lattice) are $T = -1$ eV.

The tip is also modeled as an S orbital, with a constant density of states in the whole energy range.

We consider the possible excitation of two different vibrational modes: perpendicular and parallel to the surface. The electron–vibration coupling matrix is obtained as Eq. (3). In order to keep simplicity, both modes are considered to have the same frequency and reduced mass. We set $\Delta R = 0.05$ Å, which is a typical value for molecular modes. Assuming a $1/d^2$ dependence of the hoppings with bond distance [17], the e–vib. coupling elements have a value of 0.1 eV. No distance dependence is considered for the adsorbate's level. In a general quantitative calculation, such a dependence should be present in the coupling too. The

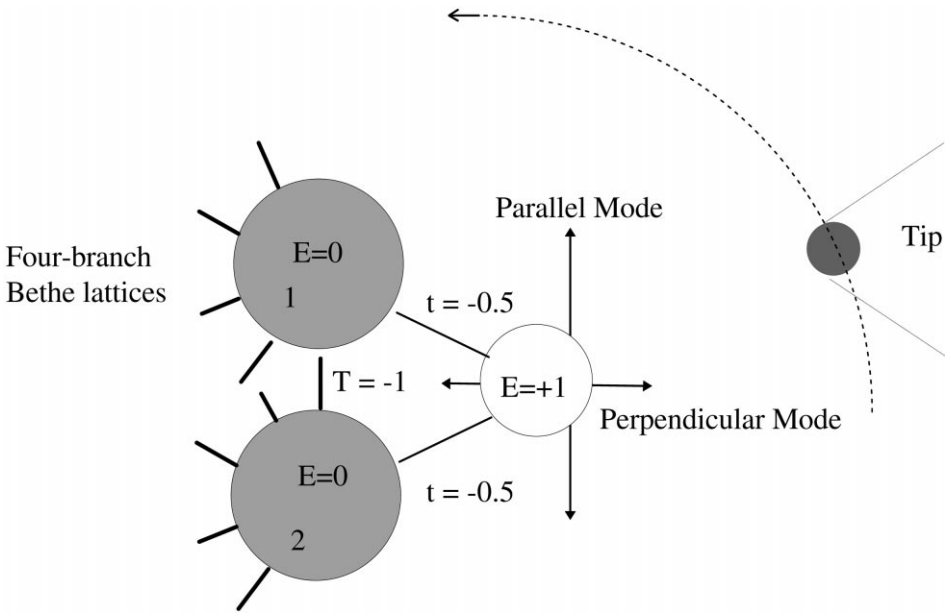

Fig. 2. Schematic illustration of the model used in the calculations. Four different positions of the tip have been considered along the dotted line, modeled as a varying hop between it and the substrate. The self-energy provided by the bulk is included by means of attaching several branches of Bethe lattices to the adsorbate's nearest neighbors.

coupling matrices are therefore:

$$V_{\text{perpendicular}} = \begin{bmatrix} 0 & 0 & 0.1 \\ 0 & 0 & 0.1 \\ 0.1 & 0.1 & 0 \end{bmatrix},$$

$$V_{\text{parallel}} = \begin{bmatrix} 0 & 0 & -0.1 \\ 0 & 0 & 0.1 \\ -0.1 & 0.1 & 0 \end{bmatrix},$$

with each of the modes. They are straightforwardly obtained from Eq. (3), where the Hamiltonian for the three atoms in the example is a 3×3 matrix (two substrate levels and the adsorbate's level in the third place).

In order not to complicate the model, we have assumed that the frequency of the modes is small enough to be approximated by zero.

We have calculated the possible excitation of up to two vibrational levels of each mode (see the schematic of Fig. 1 for the multimode excitation Hamiltonian). The inelastic current depends on the tip's position with respect to the system. We have considered four different tip positions, which would roughly represent the relative movement of the tip around the adsorbed system (see Fig. 2). For each of them, we calculate the Green's function of the total system, for the three atoms in the e–vib. island, and also the ρ matrix, which is proportional to the imaginary part of the self-energy in the Hamiltonian. Using Eq. (A8) the inelastic conductances are evaluated and integrated to obtain the corresponding currents. We show the results for excitation of one perpendicular mode, one parallel mode, two perpendicular, two parallel and one perpendicular + one parallel modes. The graphs correspond to the inelastic current normalized to the elastic one.

4. Discussion

Experiments usually do not measure directly the inelastic current, but some atomic process 'rate' which is a direct consequence of the inelastic

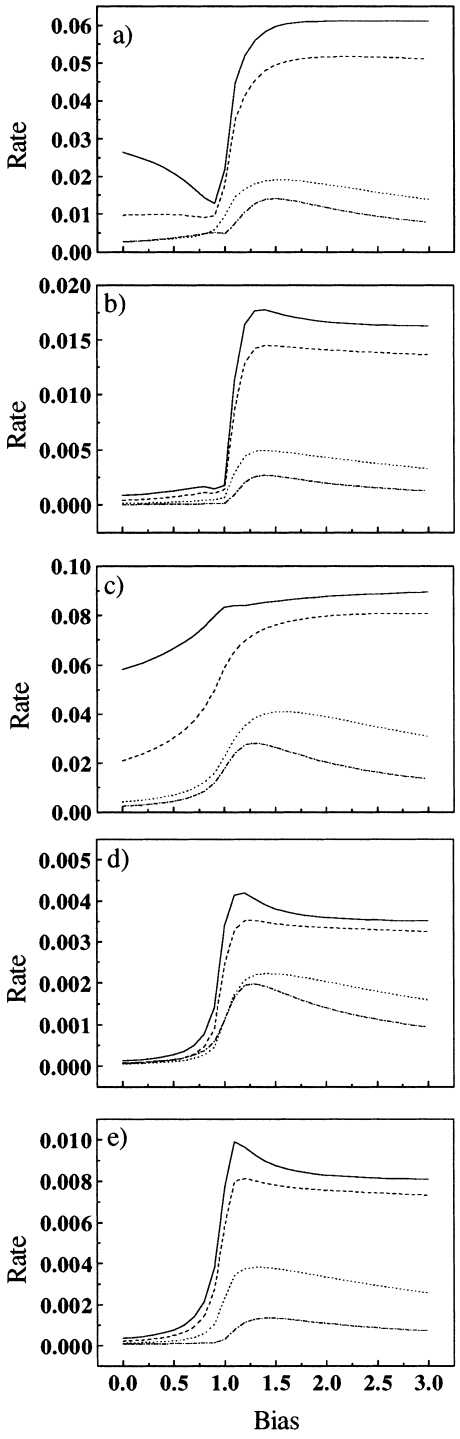

process. Such an atomic process can be, for instance, the adsorbate's desorption [1], its diffusion on the surface, or a change in its orientation [3–5]. Such processes are directly measureable, and their rates (number of events per tunneling electron) are usually explained in terms of the inelastic fraction of the current [1–5].

In the case when a single mode is dominant in the e–vib. interaction, the transition rate is proportional to the inelastic current I_N/I_0, exciting $N=\Delta E/\Omega$ levels, where ΔE is the activation barrier for the process to occur. The proportionality constant will be one if the transition takes place along the mode's vibrational coordinate. Otherwise, it is necessary to estimate the energy transfer between modes [3].

After the electron has passed, the molecule is left in a combination of vibrational modes which, in general, is not an eigenstate. Such a combination is described by its density matrix. From the Green's functions of the multibranch system shown in Fig. 1, it is easy to calculate the density matrix of the molecule after the electron has passed. This is necessary if several modes are responsible for some measurable process to occur; for instance, if both diffusion and desorption have similar activation barriers and both are likely to happen. We shall not enter into the discussion about the results of such calculations in this paper.

We thus assume that our system is such that just one of the calculated inelastic currents is provoking the measurable transition. Therefore,

Fig. 3. Inelastic currents normalized to the elastic one, as a function of the voltage. The rate is given in 'events per tunneling electron'. The bias is given in volts. Graphs correspond to: (a) $I_{1,0}/I_{0,0}$; (b) $I_{2,0}/I_{0,0}$; (c) $I_{0,1}/I_{0,0}$; (d) $I_{0,2}/I_{0,0}$; and (e) $I_{1,1}/I_{0,0}$. The indices denote the modes excited by the current: the first one is the perpendicular mode and the second is the parallel mode. The number 0, 1 or 2 indicates the number of vibrational levels of the mode which are being excited. The different lines correspond to four different positions of the tip with respect to the adsorbate. They are described by the different tip sample hopping elements. Solid line, $T_1=0$, $T_a=1$; dashed line, $T_1=0.33$, $T_a=0.66$; dotted line, $T_1=0.66$, $T_a=0.33$; dot–dash line, $T_1=1$, $T_a=0$. T_a is the hopping between the tip and the adsorbate, T_1 is that between the tip and atom 1. T_2, hopping with atom 2, is always 0 (see Fig. 2).

an STM experiment would be able to produce a plot of such a current, with bias resolution, and also spatial resolution. Let us concentrate on the spatial resolution first. Such a measurement has already been performed for the acetylene rotation process in Ref. [3]. The authors measure the transition rate per tunneling electron, as a function of the tip's position, obtaining some 'inelastic profile' of the molecule. The graphs in Fig. 3 show that the corrugation and shape of the profile can depend sensibly on the bias. Let us focus on $I_{1,0}/I_{0,0}$ and $I_{0,1}/I_{0,0}$ plots (Figs. 3a and c). The solid line corresponds to the tip just over the molecule. The other lines would represent the progressive lateral displacement of the tip with respect to that position. There is a clear threshold in the bias, due to the resonance near the adatom's energy level. For biases below the threshold, the 'events per electron' rate increases quite abruptly when the tip is near the vertical position over the molecule (it decreases to half of the rate, from the solid line to the dot–dash one), corresponding to a sharp profile. However, when the bias exceeds the threshold, the rate stays high for a wider lateral displacement, thus implying a broader profile of the 'inelastic profile' of the molecule. In the case of higher excited modes, the same phenomenon occurs (though it is difficult to appreciate the low bias rate in the graphs).

An apparent feature in the bias dependence of the transition rate is the steepness of the curve near the threshold. We can see that the more levels are excited, the steeper the curve becomes. Such a behavior is to be expected from the approximated expression Eq. (A12) for the conductance. It is the reason for the extremely abrupt dependence found experimentally in Ref. [1]. There, the authors desorbed CO molecules via inelastic tunneling. Below a threshold of 2.4 eV they could not detect any single event, while the rate increased rapidly above such a voltage. In their case the number of levels excited to produce one desorption is about 10, which implies a negligible probability for biases below the threshold. A simplistic view considering the desorption rate as proportional to the current through the π^* orbital is clearly unable to explain the abrupt dependence with bias.

Let us now comment on the validity of Eq. (A12). The deduction provided in the Appendix is valid only when the e–vib. coupling involves just one orbital. As it can be checked from the curves in Fig. 3, it is approximately fulfilled in the zero bias limit. However, its failure is clear if we compare Figs. 3a and b for $I_{1,0}/I_{0,0}$ and $I_{2,0}/I_{0,0}$: the solid line presents a negative slope for $I_{1,0}/I_{0,0}$, due to the faster increase of $I_{0,0}$ in comparison with $I_{1,0}$. According to Eq. (A12), a negative slope would be expected for $I_{2,0}/I_{0,0}$ as well; however, that is not the case. Thus, in the general case, the approximated expression Eq. (A12) does not hold. The reason for it is the many-orbital nature of the e–vib. coupling.

5. Conclusions

A Green's functions method is proposed to calculate inelastic currents in the STM, when there are many orbitals present in the electron–vibration coupling and several different modes can be simultaneously excited. The method is thus more general than presently existing approaches. By means of a model, we show how our method can predict transition rates for processes like adatom desorption, diffusion or rotation. It is shown that the spatial dependence of the rate as a function of the tip's position (the 'inelastic image' of the molecule) can present a sharper or broader shape, depending on the bias. The experimental availability of such an 'inelastic image' of the molecule has already been proved for the acetylene molecule on copper [3]; however, no systematic studies which include a bias dependence have been performed yet. An abrupt threshold in the events rate is shown to happen, which becomes more abrupt as the number of excited levels increases, in agreement with experimental results. A known power relation between the different inelastic currents, which is valid for the one-orbital case, is shown to fail when several orbitals are involved in the inelastic coupling, thus proving the need of including a multi-orbital approach like the one presented here in any realistic model of inelastic current processes. The implementation of the method described in a quantum-chemical framework like those in Refs. [15,19] is straightforward.

Acknowledgements

M. Rose, M. Salmeron, R. Perez and F. Flores are acknowledged for helpful comments. The work was supported by Grant-in-Aid for Creative Basic Research (09NP1201) from the Ministry of Education, Science, Culture and Sports of Japan. N.M. acknowledges an STF fellowship from the European Union.

Appendix A

A1. The coupled parallel systems Hamiltonian

Let us concentrate on the one-electron case. A derivation for the many-electron case is possible using the Keldysh formalism. We have checked that the main conclusions are not altered. In order to make the derivation as clear and intuitive as possible, we present just the one-electron case.

Let us consider the total stationary wave function of the electron plus oscillator as:

$$\sum_{n,k} a_{n,k}|\Psi_{n,k}\rangle\delta(E-E_k-n\Omega) = \sum_{n,k} a_{n,k}|ph_n\rangle\, e^{in\Omega t}|\psi_k\rangle\, e^{iE_k t}\delta(E-E_k-n\Omega). \quad (A1)$$

The Hamiltonian is:

$$H=\sum_k C_k^+ C_k E_k + V^+ V\Omega + c_a^+ c_a(V^+ + V)\delta\epsilon.$$

To make the expressions simpler we just consider coupling at site a, it being straightforward to make the derivation in the general case of a coupling like in Eq. (4).

In the base $|\Psi_{n,k}\rangle$, the Hamiltonian elements are:

$$H_{nk,n'k'} = (E_k + n\Omega)\delta_{nn'}\delta_{kk'} + (\sqrt{n}\delta_{n,n'+1} + \sqrt{n'}\delta_{n+1,n'})\delta\epsilon \times \langle\psi_k|a\rangle\langle a|\psi_{k'}\rangle\delta(\Omega - E_k - E_{k'}). \quad (A2)$$

The proper base for LCAO calculations is a localized orbital base. Then the Hamiltonian takes the form:

$$H_{ni,n'j} = \sum_{m,k,m',k'} \langle n,i|m,k\rangle H_{mk,m'k'}\langle m',k'|n,j\rangle = \delta_{nn'}(H_{ij}+\delta_{ij}n\Omega) + (\delta_{n,n'+1}\sqrt{n} + \delta_{n',n+1}\sqrt{n'})\delta_{ia}\delta_{ja}\delta\epsilon. \quad (A3)$$

It describes the electron propagation. This is clearly represented by Fig. 1, where the oscillator state is given by the branch in which the electron is. Thus, in general, after the electron has passed, we find the oscillator in a combination of different vibrational states, given by the probability amplitudes of the wavefunction in the different branches.

A2. Exact expression for the inelastic current

Let us assume that the electron is incident on the oscillator when it is in its ground state. Therefore the elastic conductance is given by the flux entering electrode A and exiting through electrode B in Fig. 1, while the inelastic conductance exciting n modes corresponds to the flux entering electrode A and exiting through the corresponding nth branch of the sample (Fig. 1).

The general expression for the current driven by an LCAO wavefunction between two neighboring sites is given by:

$$j_{ab}(\psi) = \frac{2e}{\hbar}\,\mathrm{Im}(\psi^*(a)T_{ab}\psi(b)), \quad (A4)$$

where T_{ab} is the Hamiltonian matrix element between the two sites (or orbitals). This follows simply from:

$$\frac{d|\psi(a)|^2}{dt} = \frac{i}{\hbar}\left(\psi_i\sum_j H_{ij}\psi_j^* - \psi_i^*\sum_j H_{ij}\psi_j\right) = \frac{2}{\hbar}\,\mathrm{Im}\left(\psi_i^*\sum_j T_{ij}\psi_j\right) \equiv \frac{1}{e}\sum_j J_{ij}. \quad (A5)$$

The language of Green's functions is much more adequate for LCAO calculations involving surface systems. Let us thus obtain the proper expressions for the conductance in terms of them. The outgoing current through electrode 2 in the multi-electrode system of Fig. A1 is:

$$\sigma = \frac{4e}{\hbar}\,\mathrm{Im}\left(\sum_p \underline{\psi}_p(a')\underline{\underline{T}}_{a'2}\bar{\psi}_p^*(2)\right), \quad (A6)$$

where a' and 2 represent two groups of orbitals which are directly connected by Hamiltonian matrix elements. $\bar{\psi}$ and $\underline{\psi}$ are arrays (vertical and horizontal) with elements corresponding to each of the orbitals in the group (a' or 2), and $\underline{\underline{T}}$ is the

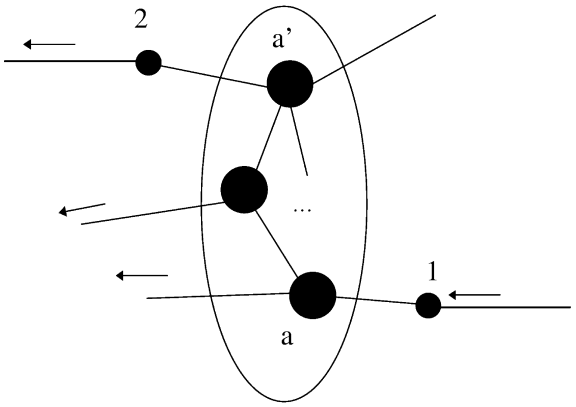

Fig. A1. Schematic illustration for the derivation in Section A2.

part of the Hamiltonian connecting the two groups. p represents the eigenfunctions incident from electrode 1 and scattered into the rest of the system. The functions satisfying such a condition (to be incident only from electrode 1) can be written as:

$$\bar{\psi}_p(a') = G_{a'a} T_{a1} \bar{\phi}_p(1), \quad \bar{\psi}_p(2) = G_{2a} T_{a1} \bar{\phi}_p(1), \tag{A7}$$

where G is the Green's function of the total system and ϕ is an eigenfunction of electrode 2 uncoupled from a'. Therefore expression (A6) can be recast as:

$$\sigma = \frac{4e}{\hbar} \operatorname{Im} \sum_{p \in F} (\phi_p^*(1) T_{1a} G_{aa'} T_{a'2} G_{2a} T_{a1} \bar{\phi}_p(1))$$

$$= \frac{8e}{\hbar} \operatorname{Tr}[\rho_1 T_{1a} G_{aa'} T_{a'2} \rho_2 T_{2a'} G_{a'a} T_{a1}], \tag{A8}$$

where we have used $G_{2a} = g_{22} T_{2a'} G_{a'a}$ (g is the Green's function of the system when the e–vib. coupling and the electrode coupling are zero). The densities of states ρ correspond to those of the uncoupled electrodes (1 or 2). The meaning of $p \in F$ is that we make the summation for the eigenfunctions p of the uncoupled electrode 1, such that their energy is within the energy interval $(E, E + \mathrm{d}E)$. This expression is equivalent to that obtained in Ref. [18] for the case of one level in the central island.

The expression obtained is well suited for LCAO calculations of the elastic and inelastic conductances for real systems involving many orbitals in the electrodes.

A3. Approximate expression for the inelastic conductance

The expression obtained enables us to very easily obtain several approximated formulas which have been derived by other authors. For the case of a single resonance and a single-vibrational-mode system, Ref. [7] gives a simple expression for the inelastic conductance exciting n quanta of vibration in terms of the total elastic and inelastic conductances. For such a case, expression (A8) is simply:

$$\sigma_n = \rho_l \rho_r T^2 |G_{0n}|^2. \tag{A9}$$

Provided the inelastic coupling term is small (as is the usual case):

$$G_{0n} = g_{00} t_{01} G_{1n},$$

$$G_{1n} = g_{11}(t_{10} G_{0n} + t_{12} G_{2n}) \approx g_{11} t_{12} G_{2n}, \tag{A10}$$

and so on. The g's are the Green's functions of the system when the e–vib. coupling is zero, and $t_{n,n+1}^2 = (n+1) t_{01}$ is the e–vib. coupling between levels n and $n+1$ of the oscillator. Furthermore, for Ω small enough, $g_{nn}(\epsilon) = g_{00}(\epsilon - n\Omega) \approx g_{00}(\epsilon)$, so:

$$|G_{0n}|^2 \approx |g_{00}|^{2n} t_{01}^{2n} n! \tag{A11}$$

Therefore:

$$\sigma_1 \approx \rho_l \rho_r T^2 t_{01}^2 |g_{00}|^2, \quad \frac{\sigma_1}{\sigma_0} \approx t_{01}^2 |g_{00}|^2,$$

$$\sigma_n \approx \sigma_0 \left(\frac{\sigma_1}{\sigma_0} \right)^n n! \tag{A12}$$

The last expression is the same as that obtained in Ref. [5]. Using our starting expression, Eq. (A8), one can easily calculate the exact one-electron inelastic conductances.

In the case of several orbitals at the interface, the above derivation is no longer valid and the relation obtained is not necessarily true, as it can be seen from the results of Section 4.

From the above expressions it is also clear that,

in the case of a Lorentzian resonance, the ratio of inelastic to zero-order elastic conductance is:

$$\frac{\sigma_1}{\sigma_0} \approx \frac{\delta\epsilon^2}{\epsilon^2+\Gamma^2}, \tag{A13}$$

using the notation of Ref. [10]. The change in elastic conductance due to the opening of the inelastic channel, up to second order in $\delta\epsilon$, normalized by the zero-order conductance at $\epsilon-\Omega$, is:

$$\frac{\delta\sigma_0^{(2)}}{\sigma_0^{(0)}} = \frac{\delta\epsilon^2}{\epsilon^2+\Gamma^2}\left(\frac{(\epsilon-\Omega)^2-\Gamma^2}{(\epsilon-\Omega)^2+\Gamma^2}\right), \tag{A14}$$

which gives a decrease in the conductance near the center of the resonance (when $\epsilon^2<\Gamma^2$) due to the opening of the inelastic channel, as predicted by Ref. [10].

References

[1] L. Bartels, G. Meyer, K.-H. Rieder, D. Velic, E. Knoesel, A. Hotzel, M. Wolf, G. Ertl, Phys. Rev. Lett. 80 (1998) 2004.

[2] B.C. Stipe, M.A. Rezaei, W. Ho, S. Gao, M. Persson, B.I. Lundqvist, Phys. Rev. Lett. 78 (1997) 4410.

[3] B.C. Stipe, M.A. Rezaei, W. Ho, Phys. Rev. Lett. 81 (1998) 1263.

[4] B.C. Stipe, M.A. Rezaei, W. Ho, Science 280 (1998) 1732.

[5] B.C. Stipe, M.A. Rezaei, W. Ho, Science 279 (1998) 1907.

[6] S. Gao, M. Persson, B.I. Lundqvist, Phys. Rev. B 55 (1997) 4825.

[7] G.P. Salam, M. Persson, R.E. Palmer, Phys. Rev. B 49 (1994) 10655.

[8] Ph. Avouris, R.E. Walkup, A.R. Rossi, H.C. Akpati, P. Nordlander, T.C. Shen, G.C. Abeln, J.W. Lyding, Surf. Sci. 363 (1996) 368.

[9] R.E. Walkup, D.M. Newns, Ph. Avouris, J. Electron Spectrosc. Relat. Phenom. 64/65 (1993) 523.

[10] B.N.J. Persson, A. Baratoff, Phys. Rev. Lett. 59 (1987) 339.

[11] J.W. Gadzuk, Phys. Rev. B 44 (1991) 13466.

[12] J.W. Gadzuk, Surf. Sci. 342 (1995) 345.

[13] K. Stokbro, B.Y.-K. Hu, C. Thirstrup, X.C. Xie, Phys. Rev. B 58 (1998) 8038.

[14] M.A. Gata, P.R. Antoniewicz, Phys. Rev. B 47 (1993) 13797.

[15] N. Mingo, L. Jurczyszyn, F.J. Garcia Vidal, R. Saiz-Pardo, P.L. de Andres, F. Flores, S.Y. Wu, W. More, Phys. Rev. B 54 (1996) 2225.

[16] R.A. Van Santen, Theoretical Heterogeneous Catalysis, World Scientific, Singapore, 1991.

[17] W.A. Harrison, Electronic Structure and the Properties of Solids, Freeman, New York, 1980.

[18] K. Makoshi, T. Mii, Jpn. J. Appl. Phys. 34 (1995) 3325.

[19] M.L. Boquet, P. Sautet, Surf. Sci. 360 (1996) 128.